Supplementary Information

Results

Generation of Atf-7$^{-/-}$ mice

Atf-7$^{-/-}$ mice were generated by homologous recombination in TT2 ES cells. The *Atf-7* gene was disrupted by replacing exon 10 (amino acids 376-413), which encodes part of the ATF-7 DNA-binding domain containing the 4th and 5th leucines of the leucine zipper structure, with the neomycin (*neo*^{r}) cassette (Supplementary Figure S1A). Homologous recombinants were characterized by the appearance of a 3.2-kb *Eco*RI fragment and a 6.5-kb *Bam*HI fragment after hybridization with a 5'- and 3'-probe, respectively (Supplementary Figures S1A and S1B). Among 720 G418-resistant ES cell colonies, 6 (0.8%) had a mutated target allele. Using standard techniques, chimeras were obtained from three independent mutant ES clones and mated with C57BL/6 females to establish three mutant mouse lines. Heterozygous (*Atf-7*$^{+/-}$) and homozygous (*Atf-7*$^{-/-}$) mice were identified by Southern blot analysis of genomic DNA isolated from tail biopsies (Supplementary Figure S1B). Crossbreeding of heterozygous mice gave the expected Mendelian ratios: of the 203 screened progeny, 50 (25%) were *Atf-7*$^{+/+}$, 101 (50%) were *Atf-7*$^{+/-}$ and 52 (25%) were *Atf-7*$^{-/-}$. The monoclonal antibody 1A7, which is directed to a sequence (aa 328-343) outside the deleted ATF-7 coding region, did not detect the 65-kD *Atf-7* gene product (ATF-7), but detected a 48-kD ATF-7 fragment in a western blot analysis of adult brain extracts from *Atf-7*$^{-/-}$ mice (Supplementary Figure S1C).

In our targeting strategy, exon 10, which encodes part of the DNA-binding

domain, was replaced with the neomycin (*neo*^{r}) cassette. This suggests that the ATF-7 fragment expressed in *Atf-7*$^{-/-}$ mice contains exons 1-9 and lacks the functional leucine zipper. To investigate whether this ATF-7 fragment affects the activity of ATF-7 or ATF-2 as a dominant-negative form, for instance by interacting with specific factor(s) via its N-terminal trans-activation domain, we examined ATF-7 and ATF-2 dependent CAT (Chloramphenicol Acetyltransferase) expression from the CRE-containing promoter in WT and *Atf-7*$^{-/-}$ MEFs (Supplementary Figure S1D). The basal expression levels from the CRE-containing promoter was 1.8-fold higher in *Atf-7*$^{-/-}$ cells compared to WT cells, indicating a role for ATF-7 in gene silencing. ATF-7 and ATF-2 repressed and activated CAT expression, respectively, to similar degrees in WT and *Atf-7*$^{-/-}$ MEFs. Furthermore, c-Jun activated CAT expression from the TRE (TPA response element)-containing promoter to a similar degree in WT and *Atf-7*$^{-/-}$ MEFs. These results suggest that the ATF-7 fragment expressed in *Atf-7*$^{-/-}$ mice does not act as a dominant-negative.

As there is much crosstalk and potential redundancy between other ATF/CREB family members, we also examined whether a loss of functional ATF-7 affects the expression levels of other ATF/CREB proteins. There was almost no difference in the levels of c-Jun, ATF-2, and CRE-BPa between WT and *Atf-7*$^{-/-}$ adult brain extracts (Supplementary Figure S1E).

Materials and methods

Generation of Atf-7*-deficient mice*

Atf-7-deficient mice were generated essentially as described previously (Maekawa et al,

1999). An *Atf-7* genomic DNA clone was isolated from a C57BL/6 mouse genomic DNA library using mouse *Atf-7* cDNA as a probe. The targeting vector was constructed by replacing a fragment encoding part of the b-ZIP DNA-binding domain with a *neo* gene cassette. The diphtheria toxin A gene (*DT-A*) was inserted for negative selection. A *Not*I-linearized targeting vector (100 μg) was introduced into 2 x 10^7 TT2 ES cells by electroporation. Targeted clones were isolated after growth in the presence of G418 (150 μg/ml) for 7 days and were then expanded in 24-well plates. Homologous recombination was confirmed by Southern blot analysis using two different probes (a 5' probe and a 3' probe). Approximately 20 ES cells per embryo were injected into 40 ICR 8-cell embryos, which were transplanted into the uterus of pseudopregnant females to produce chimeras. Chimeric mice were crossed with C57BL/6 mice and three mutant mouse lines were established.

CAT reporter assays

MEFs were prepared from embryos as described previously (Maekawa et al, 2007). To examine the ATF-7-dependent CAT expression from the CRE-containing promoter, mixtures containing 1 μg pTK-CAT-4CRE, which contained four tandem repeats of CRE linked to the thymidine kinase gene promoter, 2 μg of pact-ATF-7, and 0.5 μg pRL-SV40 as an internal control were co-transfected into MEFs using Lipofectamine Plus (Invitrogen). At 48 h post-transfection, CAT activity was measured and normalized for transfection efficiency by luciferase activity. To examine ATF-2-dependent CAT expression, 1 μg pact-ATF-2 was used instead of pact-ATF-7. To examine c-Jun-

dependent CAT expression, 1 μg of TRE-CAT, which contained four tandem repeats of TRE linked to the thymidine kinase gene promoter, and 0.5 μg RSV-c-Jun were used instead of pTK-CAT-4CRE and pact-ATF-7. Empty vectors (pact1 and RSV-vector) were used as negative controls for pact-ATF-7, pact-ATF-2 and RSV-c-Jun, respectively.

Behavioral analysis

The procedures used in the tests are described below.

1) Open field (OF) test. In Experiment 1 (Supplementary Figures S3A and S3B), individual mice with a mixed CBA (25%) x C57BL/6 (75%) genetic background were placed in a clear Plexiglas box (30 x 20 x 12 cm). The box was positioned in a frame that was mounted with infrared beams (Sannet SV-10; Tokyo Industry Co. Ltd). Beam interruptions due to movements of the mice were summed in 10-min bins over a period of 60 min.

In Experiment 2 (Supplementary Figure S2B), individual mice with a mixed CBA (25%) x C57BL/6 (75%) genetic background were placed in a white acrylic 250-cm^2 (50 cm long x 50 cm wide x 50 cm high) chamber (O'HARA & Co., Ltd.). OF analysis was performed on a Macintosh computer using Image OF (O'HARA& Co. Ltd.), a modified version of the public domain software NIH Image. Mice were placed in the center of the OF chamber and their behavior monitored at 1-min intervals for 10 min.

In Experiment 3 (Figure 1B), OF testing of C57BL/6 congenic mice was

performed using a 9 channel open field apparatus (O'Hara & Company, Ltd., Tokyo, Japan). Individual animals were introduced in a white plastic box (40 x 40 x 30 cm). A CCD camera was mounted above (50 cm high), and monitored the activity of an animal for 60 min. Data was analyzed by a commercial software Image J OF (O'Hara & Company, Ltd., Tokyo, Japan). Image J OF is a modified software based on the public domain software NIH Image J (http://rsb.info. Nih.gov/ij).

2) Elevated plus-maze test. The elevated plus-maze tests were performed using C57BL/6 congenic mice (Figure 1C). A single channel elevated plus maze (closed arms: 25 x 5 x 15 cm (H); open arms 25 x 5 x 0.3 cm (H)) was placed in a sound-proof room (2 x 2 x 2.5(H) m). The floor of each arm was made of white plastic and the walls of the closed arms and ridge of the open arms were made of clear plastic. Closed arms and open arms were arranged orthogonally 60 cm above the floor. Lighting of 70 Lux was placed above the center platform of the maze (5 x 5 cm). In the elevated plus maze test, each mouse was placed on the center platform facing an open arm, and then allowed to move freely in the maze for 5 min. The total distance traveled, % time in the open arms, number of entries into the open arm were measured as indices. The ratios of entries and time spent in the open arm were calculated (open arm/(open + closed arms)) x 100. Data were collected and analyzed using Image J EPM (O'Hara, Tokyo, Japan).

3) Rotating rod test. Motor coordination was assessed with a rotating rod apparatus (KN-75, Natsume Seisakujo Co., Ltd., Tokyo, Japan), which consisted of a plastic rod (3 cm diameter, 8 cm long) with a gritted surface flanked by two large discs (40 cm diameter) (Dunham and Miya, 1957, Ogura et al., 2001). A mouse was placed on the rod

and the rod was rotated at a speed of 0 (stationary), 5, or 10 rpm. Latency until a fall occurred was recorded for four trials at each speed.

4) Footprint test. To obtain footprints, black ink was applied to the hindpaws of each mouse and the mouse was allowed to walk forward in a narrow alley (9x10 (height) x 25 cm) on white paper.

5) Forced swimming test. A mouse was gently placed into a cylinder (diameter: 14.5 cm, height: 20 cm), which was filled with water (23 °C) to the depth of 13 cm. Swimming time was measured automatically for 10 min using a movement detection system (SCANET SV-10AQ, Toyo Industry Co., Japan) (Porsolt et al., 1978).

6) Water maze test. Spatial learning was assessed by three variants of the Morris water maze task (Morris et al., 1982) adapted for mice. The maze was a 150 cm diameter plastic pool filled to a depth of 31 cm with 23-25 °C water. Hidden-platform task: A circular transparent acrylic platform (diameter 12 cm) was submerged 1 cm below the surface of the water in the southeast quadrant throughout the hidden-platform task. Each mouse was subjected to four trials per day over 7 days. There were four starting points located at the center of each quadrant, and the mouse was dropped at a different starting point location for each of the four daily trials. A mouse was placed in the water facing the wall of the pool, but not touching it. The time taken to reach the platform (escape latency) was recorded. If the mouse found the platform within 60 sec, it was allowed to stay there for 30 sec. Mice that failed to find the platform in 60 sec were placed onto the platform by hand and remained on it for 30 sec. Probe trial: A single probe trial was carried out after the hidden-platform task had been completed. In this trial, the platform

was removed and the movement of each mouse in the pool was monitored using a computer-based video tracking system (BTA-2, Muromachi Kikai Co., Ltd., Tokyo, Japan). Each mouse was placed into the pool at the northwest position and was allowed to swim for 60 sec. Swimming path length, the number of times the platform site was crossed, and the time spent in the training (southeast) quadrant were calculated. Cue-platform task: In this task, a circular platform (diameter 12 cm) was made visible by attaching a black board (9 × 19 cm) on the platform and the mouse had to locate the visible platform. This task consisted of four trials per day for three consecutive days. The location of the platform varied among four possible places for each of the four trials daily. Each mouse was always started at the east position and was given 60 sec to locate the platform. Other procedures were the same as for the hidden-platform task.

Statistical analyses of behavior

Statistical analysis of the behavioral measurements was performed using a two-tailed Student's t-test after verification of homogeneity of variance (F-test). A repeated-measures ANOVA with genotypes as a between-subjects factor and time or trial as a within-subject factor was used for statistical analysis of the results of spontaneous locomotor activity, rotating rod performance, pre-pulse inhibition, and forced swimming. When the genotype factor was significant, a post hoc individual comparison was carried out. The statistical significance of differences between genotypes was analyzed using Student's t-test. The nonparametric Mann–Whitney U-test was used to analyze the

results of the wire-hanging and elevated-plus maze test. A value of $P < 0.05$ was considered significant.

DNA microarray analysis

Array analysis was performed as described previously (Maekawa et al, 2007). Total RNA was prepared from adult brainstem using the Trizol reagent (Invitrogen), and biotin-labeled RNAs for GeneChip analysis were prepared according to the protocol available on the Affymetrix website. The mouse Genome Array, containing more than 45,000 probe sets (Affymetrix; GeneChip® Mouse Genome 430 2.0 Array), was used for the analysis.

In situ hybridization

In situ hybridization was performed essentially as described previously (Nomura et al., 1999). A 901 bp sequence (+1753 to +2654) of mouse *Atf-7* cDNA was amplified from brainstem RNA by RT-PCR using ReverTra Ace reverse transcriptase and KOD-Plus DNA polymerase (Toyobo), and cloned into the pGEM-T Easy vector (Promega). For the *Htr5b* probe, a 661-bp DNA fragment (+1213 to +1824) of mouse *Htr5b* cDNA was similarly prepared. Using linearized plasmid DNA and a digoxigenin RNA labeling kit (Roche), the RNA probe was labeled with digoxigenin-UTP by transcription with SP6 and T3 RNA polymerase. Tissues were prepared essentially as described (Maekawa et al., 2007) with some modifications. In brief, mice were deeply anesthetized and transcardially perfused with 2 units/ml heparin in PBS, followed by 4%

paraformaldehyde (PFA) in PBS. Paraffin tissue sections were cut 7 μm thick and placed on glass slides. Slides were deparaffinized in xylene, hydrated, treated with proteinase K (10 mg/ml pre-warmed to 37 °C), incubated at room temperature for 15 min, and then fixed with 4% PFA. Sections were acetylated in triethanolamine at room temperature for 15 min. Prehybridizations were conducted in 50% formamide, 5×SSC, (pH 5.0, with citric acid) at room temperature for 1 h. Dig-labeled probes were diluted in hybridization solution (50% formamide, 5×SSC, 50 μg/ml tRNA, 1% SDS, 50 μg/ml heparin) at approximately 0.75 μg/ml, and hybridized with brain tissue for 1 day at 60 °C. Following hybridization, sections were washed twice in 50% formamide, 5×SSC, and 1% SDS, for 30 min at 70 °C, three times in 50% formamide, 2×SSC for 30 min at 70 °C, and three times in TB1 (100 mM Tis-HCl (pH 7.5), 150 mM NaCl) for 15 min at room temperature. After blocking with 1.5% blocking reagent for nucleic acid hybridization (Roche) in TB1 for 30 min at room temperature, slides were submerged in a 1/2000 dilution of alkaline phosphatase conjugated pre-absorbed sheep anti-digoxigenin Fab fragments (Roche) and incubated at 4 °C overnight. Slides were washed three times in TB1 at room temperature, twice in TB2 (100 mM Tris-HCl (pH 9.5), 100 mM NaCl, 50 mM $MgCl_2$) at room temperature, and then incubated with 340 μg/ml 4-nitro blue tetrazolium chloride and 175 μg/ml 5-bromo-4-chloro-3-indolyl-phosphate in TB2 at room temperature until color developed. The tissues were post-fixed in 4% PFA and mounted with cover slip.

Double *in situ* hybridization was performed essentially as described by Watakabe et al (2007). Brain sections were cut at 40 μm on a cryostat. The 910-bp

mouse 5-HTT probe (+79 ~ +988) and the *Htr5b* probe were labeled using digoxigenin and fluorescein, respectively. Hybridizations were performed more than 16 h at 55 °C using hybridization buffer (50% formamide, 1 X Denhardt's solution, 5 X SSC, pH 5.0, 10% dextran sulphate, 1% sarcosyl, 250 μg/ml tRNA).

Real time RT-PCR

Real-time RT-PCR was performed essentially as described previously (Maekawa et al., 2007). Total RNA was prepared from adult brainstem using the Trizol reagent (Invitrogen). Real-time RT-PCR was performed using the ABI 7500 and 9700 real-time PCR instruments and the QuantiTect Probe RT-PCR Kit (Qiagen), according to the manufacturers' instructions. The PCR conditions were 50 °C for 30 min, 95 °C for 10 min, and 50 cycles of 95 °C for 15 s and 60 °C for 1 min. Oligonucleotide primers and probes are shown in Supplementary Table S2.

Gel mobility-shift assays

The gel mobility-shift assays were performed essentially as described (Maekawa et al., 2008). Nuclear extracts were prepared as described by Dignam et al. from 293 T cells (5 x 10^5 cells per 10-cm dish) transfected with 10 μg of the Flag-ATF-7 expression plasmid or the control empty vector using Lipofectamine Plus (Invitrogen). Nuclear extracts were incubated for 10 min at 25 °C with 1 ng of ^{32}P-labeled DNA probe and 3 μg of poly(dI-dC) in 15 μl of binding buffer (10 mM Tris-HCl, pH 7.5, 50 mM KCl, 1 mM DTT, 0.05% Nonidet P-40, 100 μg/ml bovine serum albumin, 5% (v/v) glycerol).

The samples were then loaded onto a 4% polyacrylamide gel in 0.25% TBE (25 mM Trizma base, 25 mM boric acid, 1 mM EDTA), electrophoresed and analyzed by autoradiography. Nine ^{32}P-labeled DNA fragments, which cover the 5'-region of the mouse *Htr5b* gene, were prepared and used as probes (Supplementary Table S3). The 54-bp (-3385 to –3332) and 18-bp oligonucleotides (-2333 to –2316) containing the CRE-like sequences, which were derived from probes #2 and #4, respectively, were also used as probes (Supplementary Table S3). For competition assays, a 50-fold excess of competitor was added. The DNA sequences of mutant competitors are shown in Supplementary Table S3. In some cases, 1 μg of anti-Flag M2 antibody was added.

Western blot analysis

Extracts were prepared from embryonic day 13.5 mouse brains, adult mouse brainstems, and the nuclei of RN46A cells using a lysis buffer consisting of 20 mM Hepes (pH 7.9), 25% (vol/vol) glycerol, 420 mM NaCl, 1.5 mM $MgCl_2$, 0.2 mM EDTA, 0.5 mM DTT, 0.5 mM phenylmethylsulfonyl fluoride, 50 mM NaF, 2 mM sodium orthovanadate, 0.1 μM okadaic acid, and 25 mM β-glycerophosphate, as described (Tanaka et al. 1997). Extracts were used for western blotting. To detect P-ATF-7/2 in the brainstem extracts of the isolation-reared mice (Figure 7B), the brainstem of mice treated with a PFA perfusion were washed several times with ice-cold PBS and a nuclear extract was prepared as described by Dignam et al (1983). Protein phosphatase inhibitors (50 mM NaF, 2 mM sodium orthovanadate, 0.1 μM okadaic acid, 25 mM β-glycerophosphate) were added to all the solutions. Extracts were then boiled for 25 min in crosslinking

reversal solution (250 mM Tris-HCl, pH 8.8, 2% SDS, 0.5 M 2-mercaptoethanol) as described by Déjardin and Kingston (2009), and analyzed by SDS-PAGE. ATF-7 was detected with the anti-ATF-7 monoclonal antibody 1A7 and a peroxidase-conjugated rabbit anti-mouse κ light chain secondary antibody (Zymed), followed by ECL detection (Amersham) according to the manufacturer's instructions. To detect ATF-7 phosphorylated at Thr-53 and ATF-2 phosphorylated at Thr-71, a rabbit polyclonal antibody (Cell Signaling, #9221) which recognizes both Thr-69/Thr-71 dually phosphorylated ATF-2 and Thr-71 phosphorylated ATF-2 was used. A rabbit anti-ATF-2 polyclonal antibody (N-96 and C-19, Santa CruZ, sc-623 and sc-187) was used to detect ATF-2. The density of each band was measured with Image J software.

REFERENCES

Déjardin J, Kingston RE (2009). Purification of proteins associated with specific genomic Loci. *Cell* **136:** 175-186

Dignam JD, Lebovitz RM, Roeder RG (1983) Accurate transcription initiation by RNA polymerase II in a soluble extract from isolated mammalian nuclei. *Nucleic Acids Res* **11:** 1475-1489

Dunham NW, Miya TS (1957) A note on a simple apparatus for detecting neurological deficit in rats and mice. *J Am Pharm Assoc* **46:** 208-209.

Maekawa T, Sano Y, Shinagawa T, Rahman Z, Sakuma T, Nomura S, Licht JD, Ishii S (2008) ATF-2 controls transcription of Maspin and *GADD45a* genes independently from p53 to suppress mammary tumors. *Oncogene* **27:** 1045-1054

Morris RGM, Garrud P, Rawlins JNP, O'Keefe J (1982) Place navigtion impaired in rats with hippocampal lesions. *Nature* **297:** 681-683.

Nomura T, Khan MM, Kaul SC, Dong HD, Wadhwa R, Colmenares C, Kohno I, Ishii S (1999) Ski is a component of the histone deacetylase complex required for transcriptional repression by Mad and thyroid hormone receptor. *Genes Dev* **13:** 412-423

Ogura H, Matsumoto M, Mikoshiba K (2001) Motor disordination in mutant mice heterozygous for the type 1 inositol 1,4,5-trisphosphate receptor. *Behav Brain Res* **122:** 215-219.

Porsolt RD, Anton G, Blavet N, Jalfre M (1978) Behavioral despair in rats: a new model sensitive to antidepressant treatments. *Eur J Pharmacol* **47:** 379-391.

Tanaka Y, Naruse I, Maekawa T, Masuya H, Shiroishi T, Ishii S (1997) Abnormal

skeletal patterning in embryos lacking a single *Cbp* allele: a partial similarity with Rubinstein-Taybi syndrome. *Proc Natl Acad Sci USA* **94:** 10215-10220

Watakabe A, Ichinohe N, Ohsawa S, Hashikawa T, Komatsu Y, Rockland KS, Yamamori T (2007). Comparative analysis of layer-specific genes in Mammalian neocortex. *Cereb Cortex* **17:** 1918-1933.

Supplementary Figure legends

Supplementary Figure S1. Generation of *Atf-7*-deficient mice. **(A)** Schematic representation of the mouse *Atf-7* gene, the targeting vector, and the predicted disrupted allele. The probes used for Southern blot analyses are shown together with the predicted sizes of the hybridizing fragments. Restriction enzymes: B, *Bgl*II; BH, *Bam*HI; E, *Eco*RI; H, *Hin*dIII; X, *Xba*I. Black and shaded boxes indicate the exon regions encoding the protein-coding and 3'-untranslated region, respectively. The gray box indicates the PGK-neo cassette. **(B)** Southern blot analysis of genomic DNA extracted from the tails of wild-type (WT), *Atf-7*$^{+/-}$, and *Atf-7*$^{-/-}$ mice. (Left panel) Genomic DNA digested with *Eco*RI was hybridized with the 5' probe to yield 5.1-kb and 3.2-kb bands, representing the WT and targeted alleles, respectively. (Right panel) Genomic DNA digested with *Bam*HI was hybridized with the 3' probe to yield 9.9-kb and 6.5-kb bands, representing the WT and targeted alleles, respectively. **(C)** Immunodetection of ATF-7. Nuclear extracts from adult brains of WT, *Atf-7*$^{+/-}$, or *Atf-7*$^{-/-}$ mice were used for immunoblotting with anti-ATF-7. Equal amounts (40 μg) of nuclear extracts were loaded in each lane. **(D)** The ATF-7 fragment expressed in *Atf-7*$^{-/-}$ mice does not affect the activity of ATF-7 and ATF-2. Effect of ATF-7, ATF-2, or c-Jun on CAT expression from the CRE- or TRE-containing promoter was examined using WT and *Atf-7*$^{-/-}$ MEFs. The CAT activities relative to that in WT cells not expressing ATF-7/2 or c-Jun are shown. Values indicate mean $\pm$ SD (n = 3). **(E)** No significant difference in the levels of ATF-2, CRE-BPa, and c-Jun between WT and *Atf-7*$^{-/-}$ brain. Nuclear extracts (20 μg) of WT, *Atf-7*$^{+/-}$,

and *Atf-7*$^{-/-}$ adult brain were used for western blotting to detect the proteins indicated on the right.

Supplementary Figure S2. Abnormal behaviors of *Atf-7*$^{-/-}$ mice. Wild-type (WT; +/+) and *Atf-7*$^{-/-}$ littermate mice with a mixed CBA (25%) x C57BL/6 (75%) genetic background were use for all assays. Data are mean ± SEM. **(A)** Marble-burying test. *, $P < 0.05$ (n = 6 for each group). **(B)** Center of the open field test. Time spent in the center of the test apparatus is expressed as the percent of total time (10 min). N.S., no significant difference (n = 5 for each group). **(C)** Acoustic startle response. Amplitude of the startle response to each acoustic stimuli (non-stimulation (NS), 80, 90, 100, 110, 120 dB) is shown. *, $P < 0.05$; **, $P < 0.01$ (n = 6 and 9 for WT and *Atf-7*$^{-/-}$, respectively). **(D)** Prepulse inhibition of the acoustic startle response. The response to white noise stimuli of 120 dB following a 20 msec pre-pulse warning stimulus (70 or 80 dB) is shown. *, $P < 0.05$ (n = 6 and 9 for WT and *Atf-7*$^{-/-}$, respectively).

Supplementary Figure S3. Motor activity, motor coordination ability, and motor learning. WT and *Atf-7*$^{-/-}$ littermate mice with a mixed CBA (25%) x C57BL/6 (75%) genetic background were used for all assays. Data are mean ± SEM. **(A** and **B)** Spontaneous motor activity in a new environment. Locomotor activity was measured by infrared beam breaks. No significant difference was observed between WT and *Atf-7*$^{-/-}$ mice (n = 9 for each group). **(C)** Motor coordination ability. The test was performed using a rotating rod with a test duration of 120 sec for each trial. Retention time on the

rod was measured. No significant difference was observed between WT and *Atf-7*$^{-/-}$ mice (n = 9 for each group). **(D)** Motor learning test. The test was performed using the rotating rod at a speed of 20 rpm and 120 sec duration for each trial. Retention time on the rod was measured. No significant difference was observed between WT and *Atf-7*$^{-/-}$ mice (n = 9 for each group). **(E)** Footprint test. No significant difference was observed between WT and *Atf-7*$^{-/-}$ mice (n = 9 for each group).

Supplementary Figure S4. Forced swimming and Morris water maze tests. WT and *Atf-7*$^{-/-}$ littermate mice with a mixed CBA (25%) x C57BL/6 (75%) genetic background were use for all assays. Data are mean ± SEM. (**A**) Forced swimming test. No significant difference was observed between WT and *Atf-7*$^{-/-}$ mice (n = 10 for each group). **(B)** Escape latency for the visual platform task. Mean escape latencies over three days of testing is shown. No significant difference was observed between WT and *Atf-7*$^{-/-}$ mice (n = 5 and 9, respectively). **(C)** Escape latency for the hidden platform task. Mean escape latencies over seven days of testing is shown. No significant difference was observed between WT and *Atf-7*$^{-/-}$ mice (n = 5 and 9, respectively). **(D-F)** Probe test after acquisition of the hidden platform task. Mice swam freely for 1 min in a water maze with a platform in a trained quadrant. Time spent in each quadrant of the water maze (D), platform crossings (E), and swimming distance during the probe trial (F) are shown. SE (south-east) was the trained quadrant. No significant differences were observed between WT and *Atf-7*$^{-/-}$ mice (n = 5 and 9, respectively).

Supplementary Figure S5. *Atf-7* mRNA expression in *Atf-7*$^{-/-}$ brain. *Atf-7* mRNA expression in various brain regions of WT and *Atf-7*$^{-/-}$ mice was examined by *in situ* hybridization with anti-sense or sense probes. The data of WT mice are same as those in Figure 2A. Bar, 100 μm.

Supplementary Figure S6. Lower magnification images of *in situ* hybridization of the *Htr5b* (green) and serotonin transporter (5-HTT, red) mRNAs. Experiments were performed as described in Figures 2D and 6C using group-reared WT (A) and *Atf-7*$^{-/-}$ (B) mice, and isolation-reared WT mice (C). The images in Figures 32D and 6C were obtained using a 20x objective lens, while images using a 10x or 5x objective lens are shown here. Bar, 100 μm and 200 μm in the images using the 10x and 5x objective lens, respectively. Note that the signals using 5x objective lens were weaker than those using the 10x lens, so the 5-HTT signals were not clearly visible using the 5x objective lens. Large brain sections were partly damaged during double in situ hybridization steps, and some gaps indicated by asterisks were observed in low magnification images. *Htr5b* mRNA was predominantly detected only in the dorsal raphe nuclei of and *Atf-7*$^{-/-}$ mice and isolation-reared WT mice. 5-HTT was also detected in the dorsal raphe nuclei of these mice.

Supplementary Figure S7. *Htr5b* mRNA levels in other brain regions are unchanged. *Htr5b* mRNA expression in the indicated brain regions was examined by *in situ* hybridization. There is no obvious difference in the *Htr5b* mRNA signals between WT

and *Atf-7*$^{-/-}$ mice.

Supplementary Figure S8. ATF-7 does not bind to DNA fragments containing no CRE-like sequence in the *Htr5b* promoter region. Gel mobility-shift assays were performed using probes other than #2 and #4, as described in Figure 3B. No retarded bands were observed, indicating that ATF-7 does not bind to these promoter sequences.

Supplementary Figure S9. (A) ChIP assays were performed using the brainstem of WT and *Atf-7*$^{-/-}$ mice, and anti-histone H3-K9m3. Extracted DNA was amplified by real-time PCR using primers that cover the CRE-like sites, the transcription start site, or the 2nd exon of the *Htr5b* gene. The relative densities of bands are indicated, and each bar represents the mean $\pm$ SD (n = 3). **(B** and **C)** ChIP assays were performed using parental RN46A cells and ATF-7 kd-RN46A cells, and anti-ATF-7 (B) or anti-ATF-2 (C). Extracted DNA was amplified by real-time PCR using primers that cover the CRE-like sites, the transcription start site, or the 2nd exon of the *Htr5b* gene. The relative densities of bands are indicated, and each bar represents the mean $\pm$ SD (n = 3).

Supplementary Figure S10. Confirmation of the ATF-7 band. Equal amounts (40 μg) of nuclear extracts from WT or *Atf-7*$^{-/-}$ whole brain were used for western blotting using polyclonal antibodies which recognize both ATF-2 and ATF-7 (N96, Santa CruZ, sc-6233). Note that the band just below the ATF-2 band corresponds to ATF-7, which is absent in *Atf-7*$^{-/-}$ cells.

Supplementary Figure S11. ChIP assays were performed using the brainstem of group-reared and isolation-reared WT mice, and anti-histone H3-K9m3. Extracted DNA was amplified by real-time PCR using primers that cover the CRE-like sites, the transcription start site, or the 2nd exon of the *Htr5b* gene. The relative densities of bands are indicated, and each bar represents the mean $\pm$ SD (n = 3). **, $P < 0.01$; N.S., no significant difference.

Supplementary Figure S12. Expression of 5-HT receptors in the brain of WT and *Atf-7*$^{-/-}$ mice. Real-time RT-PCR analysis of the indicated 5-HT receptor mRNAs was performed using RNAs from the hypothalamus (upper), the cortex (middle), and the brain stem (lower). Values indicate mean $\pm$ SD (n = 4). *, $P < 0.05$; **, $P < 0.01$; ***, $P < 0.001$. N.S., no significant difference.

Supplementary Table S1. Primers and probes used for real-time (TaqMan) RT-PCR in ChIP assays.

	Forward primer	Reverse primer	TaqMan probe
Rat Htr5b cre	5'- AAACATGATCACACTGAAGATCT-3'	5'- GTGATGGGGATAAAGTCAGATGGAG-3'	5'(FAM)- TCGCACATAGCAAGAGCTGCCA-(TAMRA)3'
Rat Htr5b plus1	5'- GCTGGTACAGCGCTACAGCTACA-3'	5'- CCCTGGTTGGTTGCTGGAA-3'	5'(FAM)- AAACTCCTCCGCCCACT-(TAMRA)3'
Rat Htr5b 2nd exon	5'- GGGCCTGGAATGTTGAGTTC-3'	5'- CGCGTAGAAGGCATGGATGT-3'	5'(FAM)- CACGAAGGTAGACAACGGTTTGGCAAA-(TAMRA)3'
Mouse Htr5b cre	5'- TCTAGGCAGGGAGCTGTAAAGAG-3'	5'-GTGATGGAAATAGAGTCGGGTAAAG -3'	5'(FAM)- CTGCACGGTGTGAGCTGCCA-(TAMRA)3'
Mouse Htr5b plus1	5'- ACACGAGGAGCCCTTTGGTT-3'	5'- TGCCCAGCGCATCAAAC-3'	5'(FAM)- CCAGTCCCCAATCCTCTGCAGTC-(TAMRA)3'
Mouse Htr5b 2nd exon	5'- CCTGAAGCTTTGATAAAACGTGTTC-3'	5'- GCCTTCACCTACTGAGCCATCT-3'	5'(FAM)- ACGCAGGTGTCTTC-(TAMRA)3'

Supplementary Table S2. Primers and Probes Used for Real-time (TaqMan) RT-PCR.

	Forward primer	Reverse primer	TaqMan probe
Htr1a	5'-GAATCCGCAAGACGGTCAAG -3'	5'- CCGACGATGTTCCGAAGCT-3'	5'(FAM)- AGGTGGAAAAGAAGGGAGCGGGC-(TAMRA)3'
Htr1b	5'-AGCTACACACCCCGGCTAACT -3'	5'-GATGGACACGAGCAGGTCAGT -3'	5'(FAM)-CCTGATCGCCTCTCTGGCAGT-(TAMRA)3'
Htr2a	5'-ACCATGCGACAGGCAAGTC-3'	5'-AGCAGCCGAGGAACTTACATTC-3'	5'(FAM)- CAGGATAGCGGACCCTGGCGACA-(TAMRA)3'
Htr2c	5'-GCTGCAGTTATAAGCCAGACAA -3'	5'-GCTCCCTCCCAGACAAAGC -3'	5'(FAM)-AAGCCTCCTGTTCGACAGATTCCTAGGGT-(TAMRA)3'
Htr3a	5'- AAGCCTCGCTGAGACCATCTT-3'	5'-GTCAGGTACTGGCCGCTGTAG -3'	5'(FAM)-TGTGCGGCTGGTGCATAAGCAGG-(TAMRA)3'
Htr5b	5'- CCTGGCGGGAGCAGAAG-3'	5'-GCAGAAACACGCCAATCAAG -3'	5'(FAM)-CGGGCAGCCATGATGGTCGG-(TAMRA)3'
Cntfr	5'-CGGTGCCCACACTTTTCAGT -3'	5'-GCACAAACACGCCAATCAAG -3'	5'(FAM)-CTTCCACCTTTGCCCCTGTTTTGTACGA-(TAMRA)3'

Supplementary Table S3. DNA Probes Used for Gel Mobility-shift Assays.

Probe	Nucleotide position[1)] or sequence[2)]
#1	Nucleotides -4182to –3567
#2	Nucleotides -3566to -3241
#3	Nucleotides -3240 to –2618
#4	Nucleotides -2617 to –2281
#5	Nucleotides -2280 to –1758
#6	Nucleotides -1757 to –1097
#7	Nucleotides -1032 to –556
#8	Nucleotides -555 to –219
#9	Nucleotides -418 to +243
#2 Oligo	5′-GAGCACTTAGGGGTCGTCAGCACTTAGGGGTCTTGAGCACTTAGGGGTCGTCAG- 3′
Mutated #2 Oligo	5′-GAGCACTTAGGGGTAAACAGCACTTAGGGGTCTTGAGCACTTAGGGGTAAACAG- 3′
#4 Oligo	5′-CTCATTGCTGATGTCAAC- 3′
Mutated #4 Oligo	5′- CTCATTGCTGATAAAAAC - 3′

1) In the nucleotide numbering system used here, +1 is the transcriptional start site.

2) The CRE-like sequences and their mutated sequences are underlined.

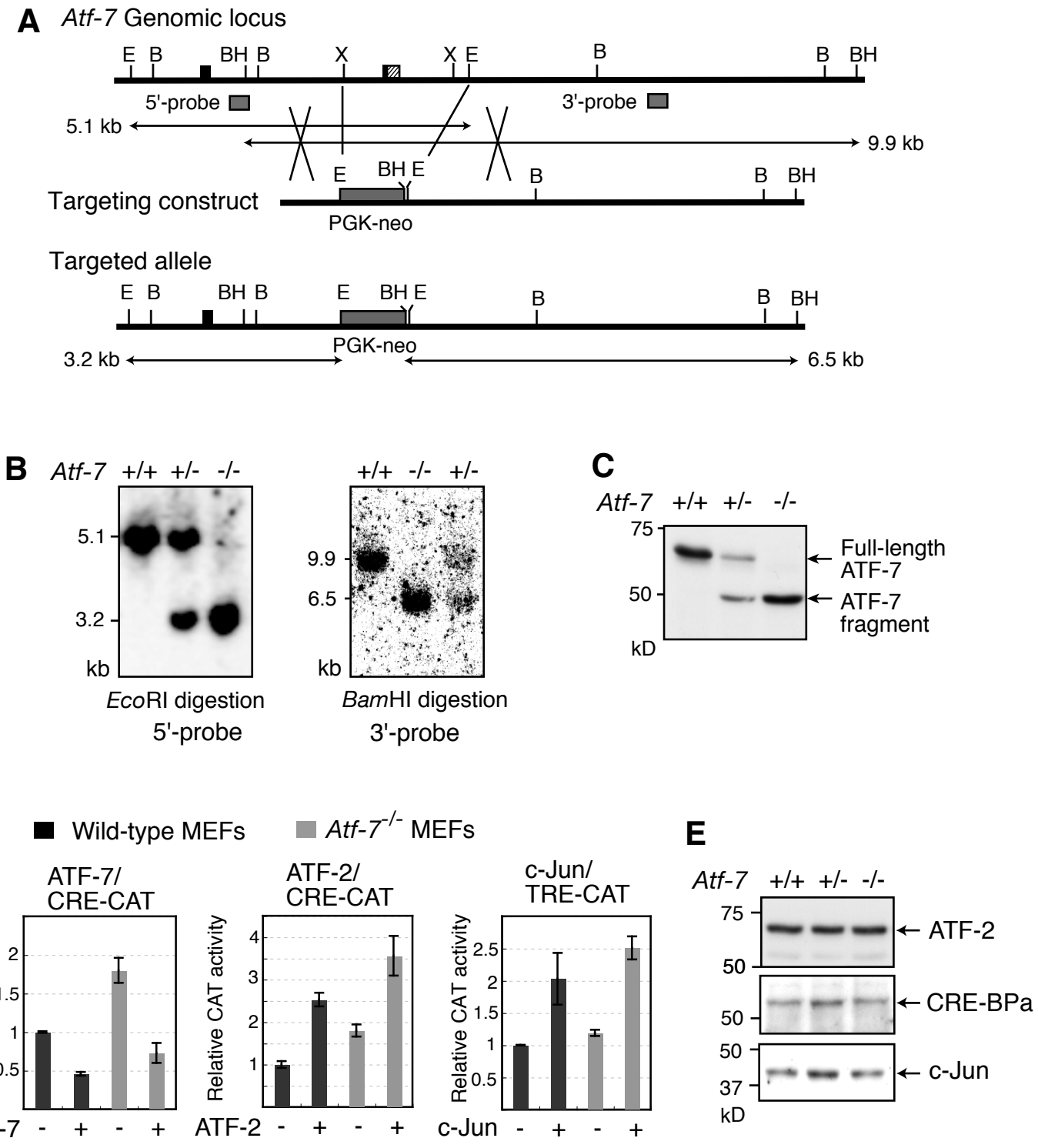
A
Atf-7 Genomic locus
E B BH B X X E B B BH
5'-probe
3'-probe
5.1 kb
9.9 kb
E BH E B B BH
Targeting construct
PGK-neo
Targeted allele
E B BH B E BH E B B BH
PGK-neo
3.2 kb
6.5 kb
B
Atf-7 +/+ +/- -/-
5.1
3.2
kb
EcoRI digestion
5'-probe
+/+ -/- +/-
9.9
6.5
kb
BamHI digestion
3'-probe
C
Atf-7 +/+ +/- -/-
75
50
kD
Full-length ATF-7
ATF-7 fragment
D
Wild-type MEFs
Atf-7-/- MEFs
ATF-7/ CRE-CAT
ATF-2/ CRE-CAT
c-Jun/ TRE-CAT
Relative CAT activity
ATF-7 - + - +
ATF-2 - + - +
c-Jun - + - +
E
Atf-7 +/+ +/- -/-
75
50
ATF-2
50
CRE-BPa
50
37
c-Jun
kD

Supplementary Fig. S2. Maekawa, T. *et al.*

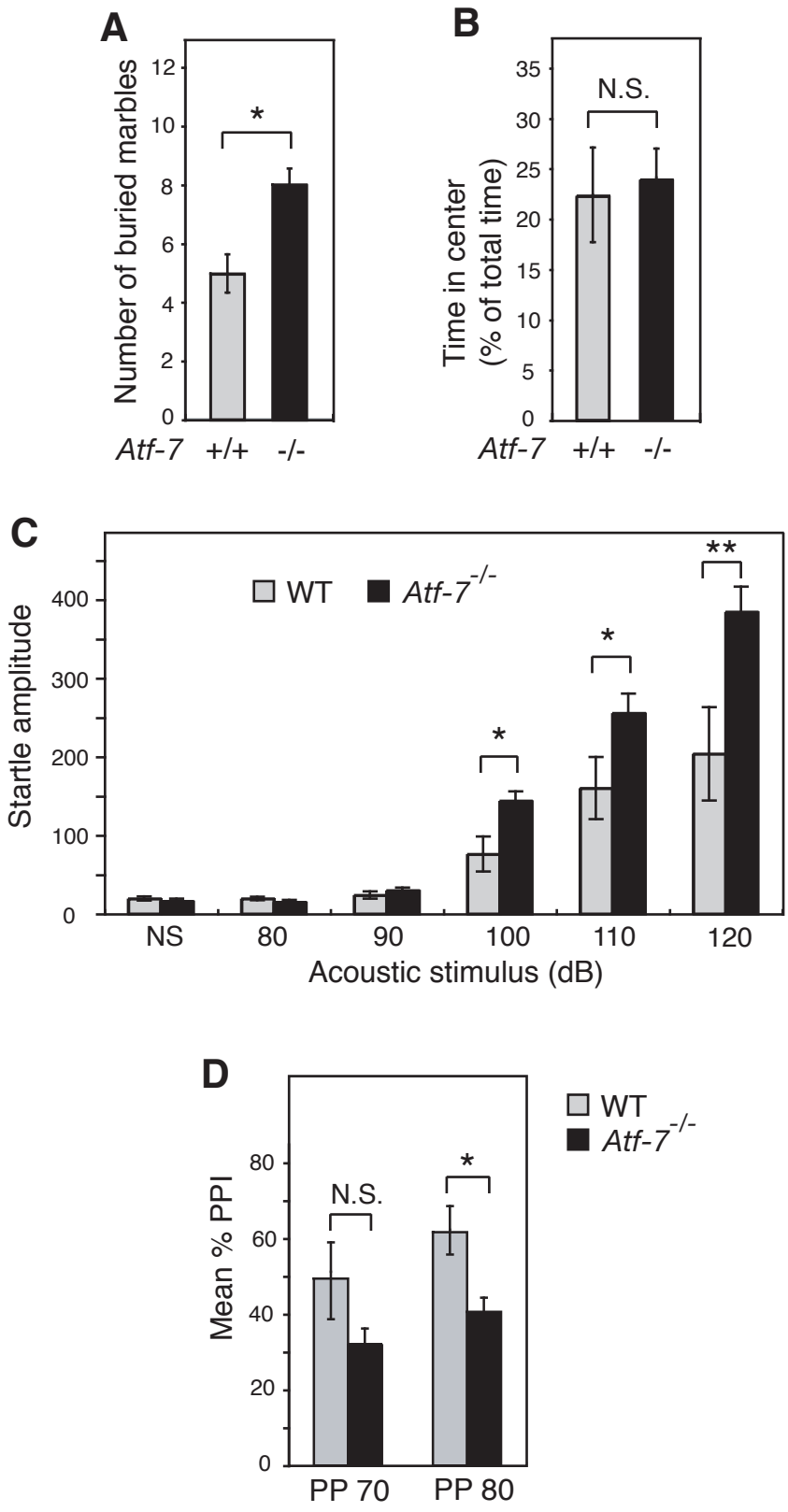

Supplementary Fig. S3. Maekawa, T. *et al*.

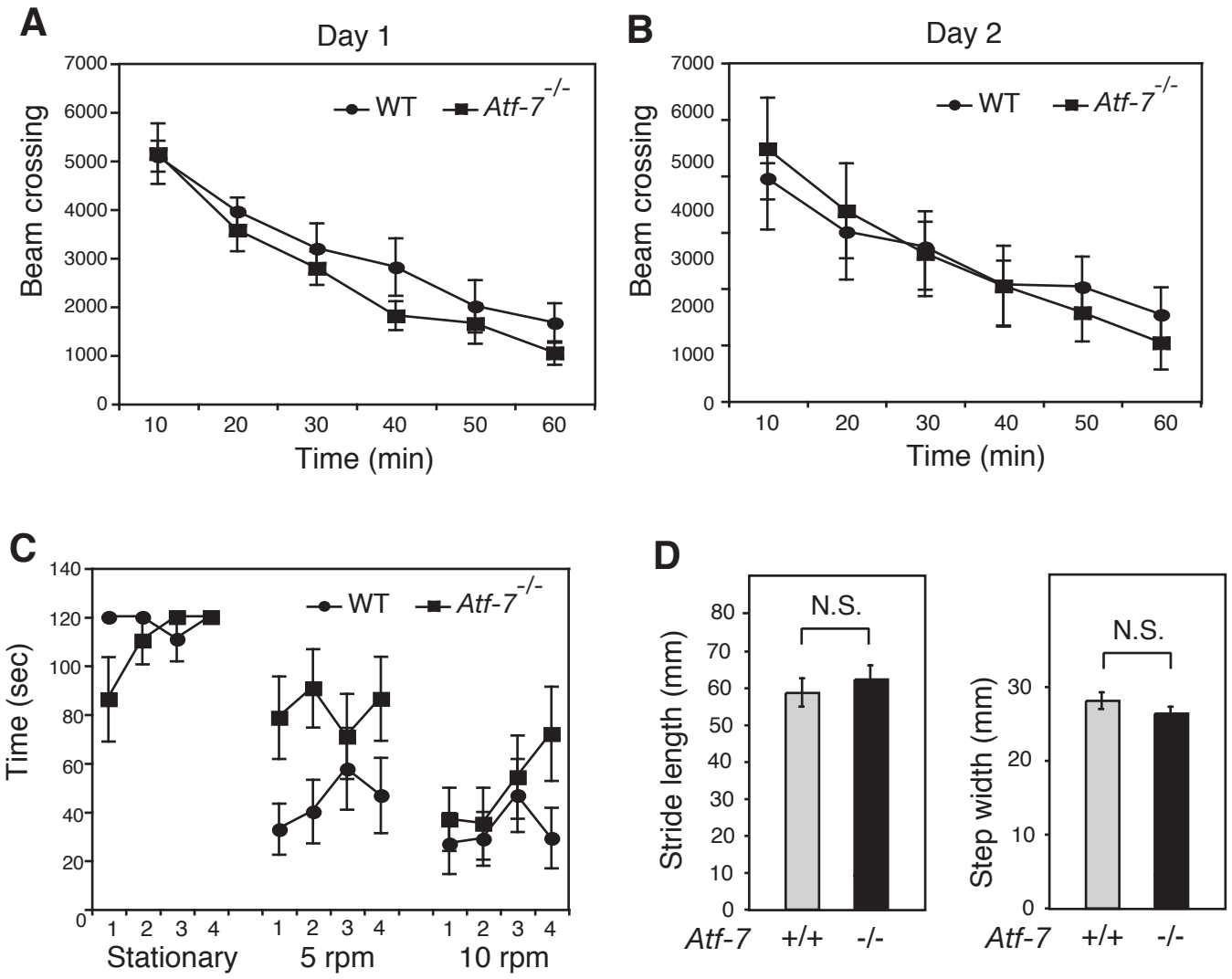

Supplementary Fig. S4. Maekawa, T. *et al*.

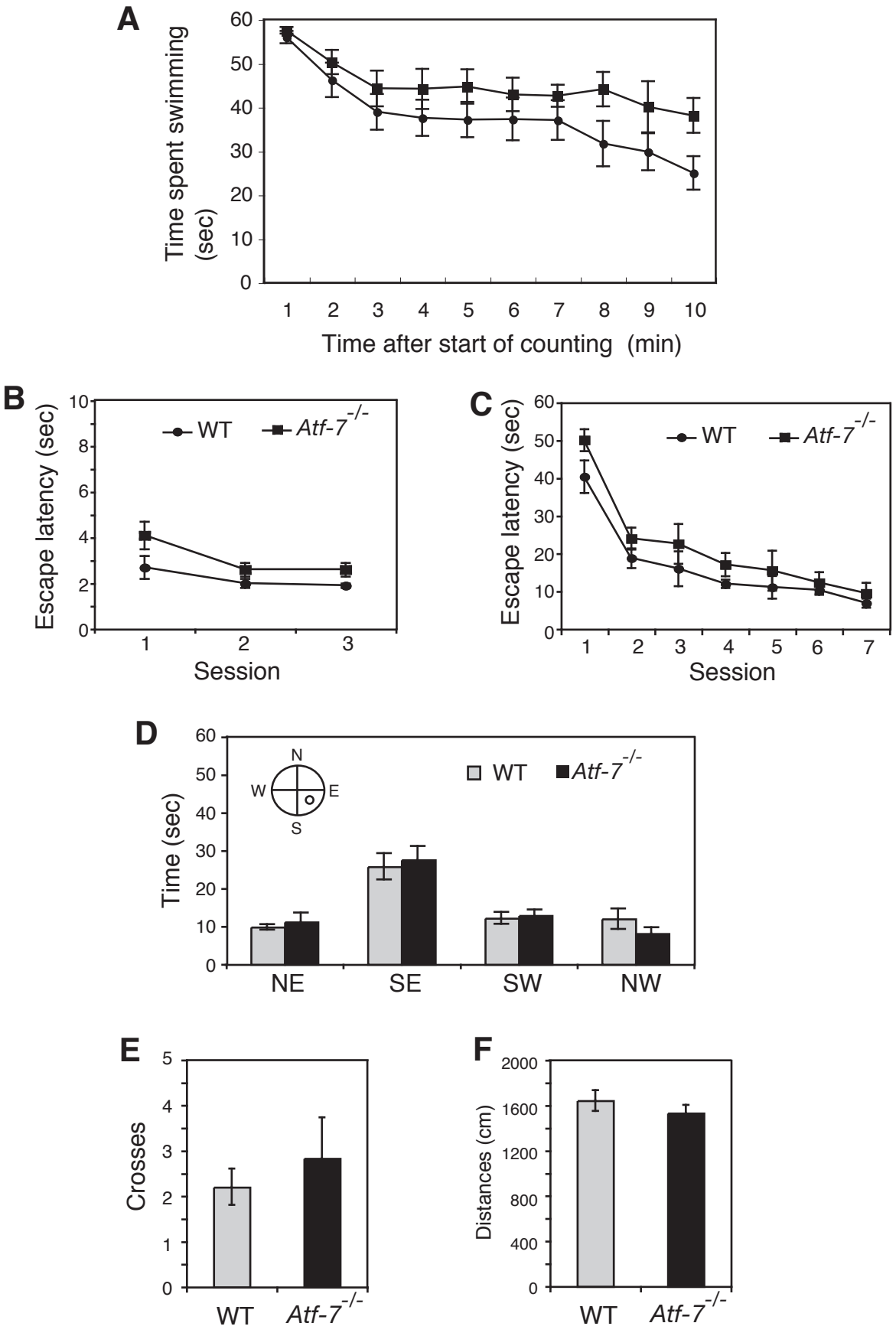

Supplementary Fig. S5. Maekawa, T. *et al.*

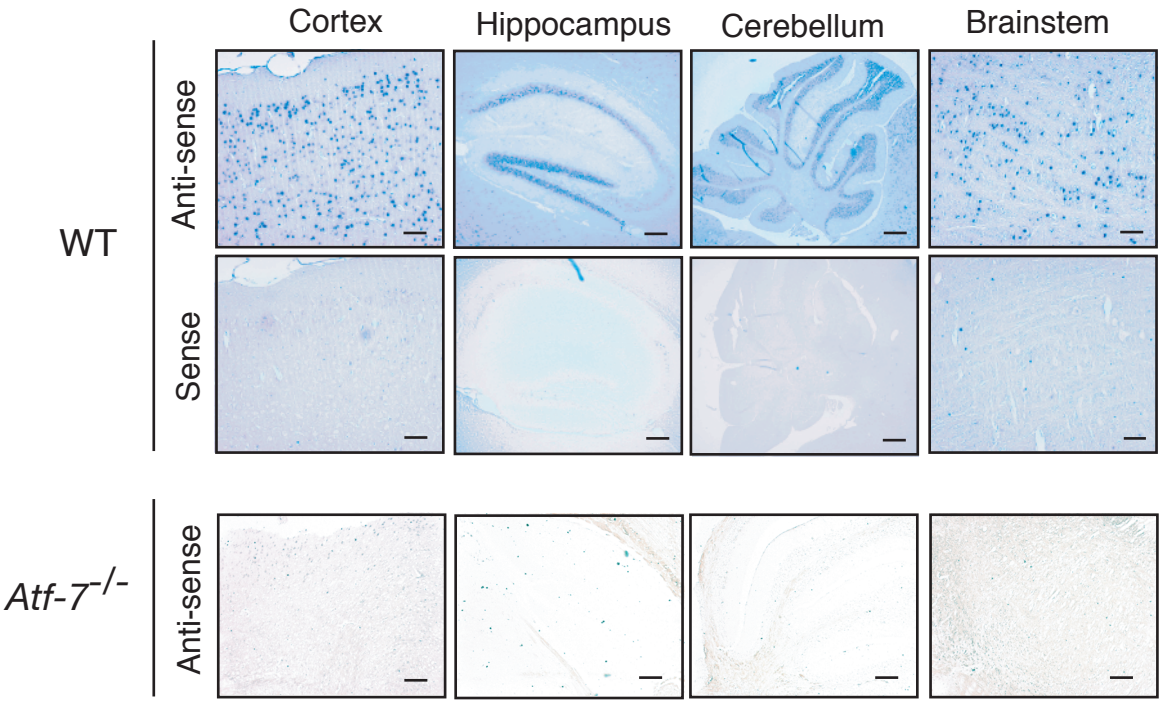

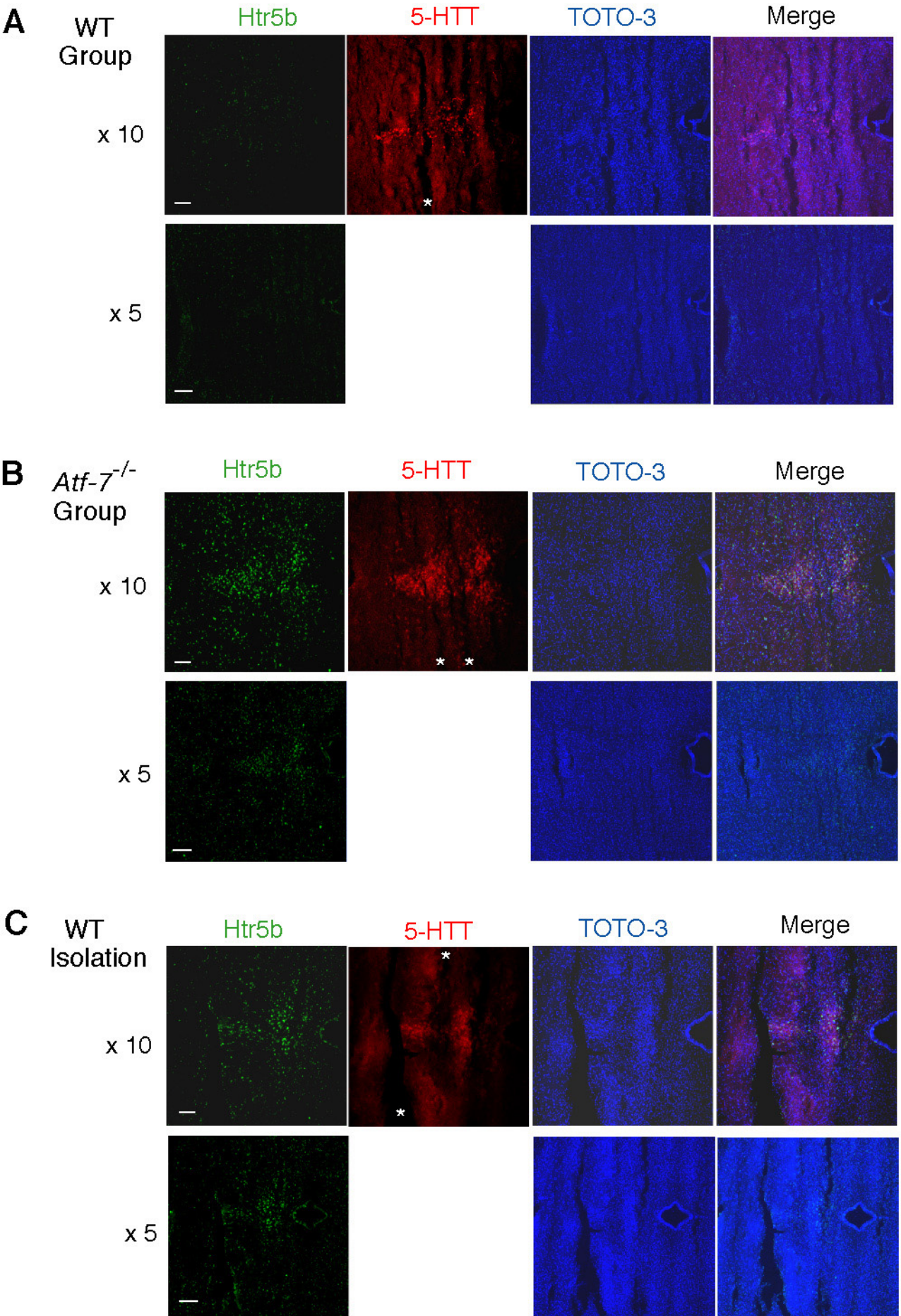
A
WT
Group
Htr5b
5-HTT
TOTO-3
Merge
x 10
x 5
B
Atf-7-/-
Group
Htr5b
5-HTT
TOTO-3
Merge
x 10
x 5
C
WT
Isolation
Htr5b
5-HTT
TOTO-3
Merge
x 10
x 5

Supplementary Fig. S7. Maekawa, T. *et al*.

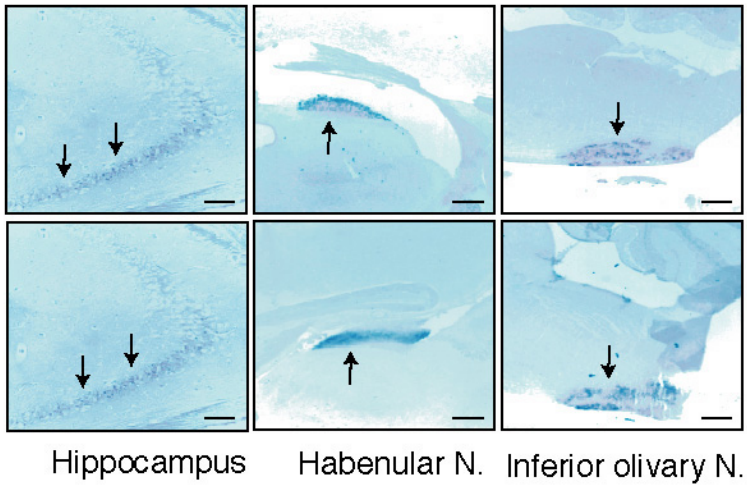

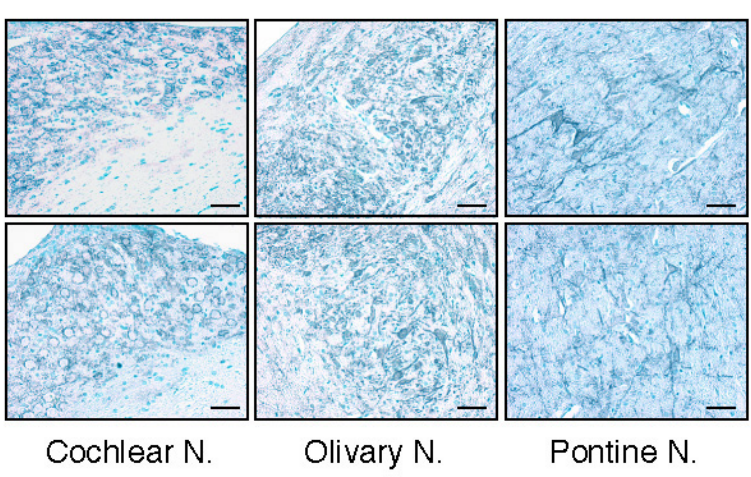

Supplementary Fig. S8. Maekawa, T. *et al*.

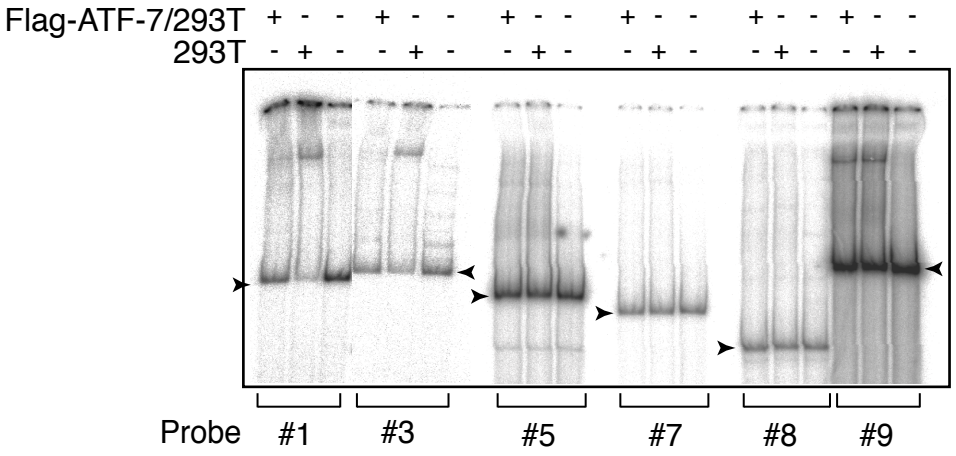

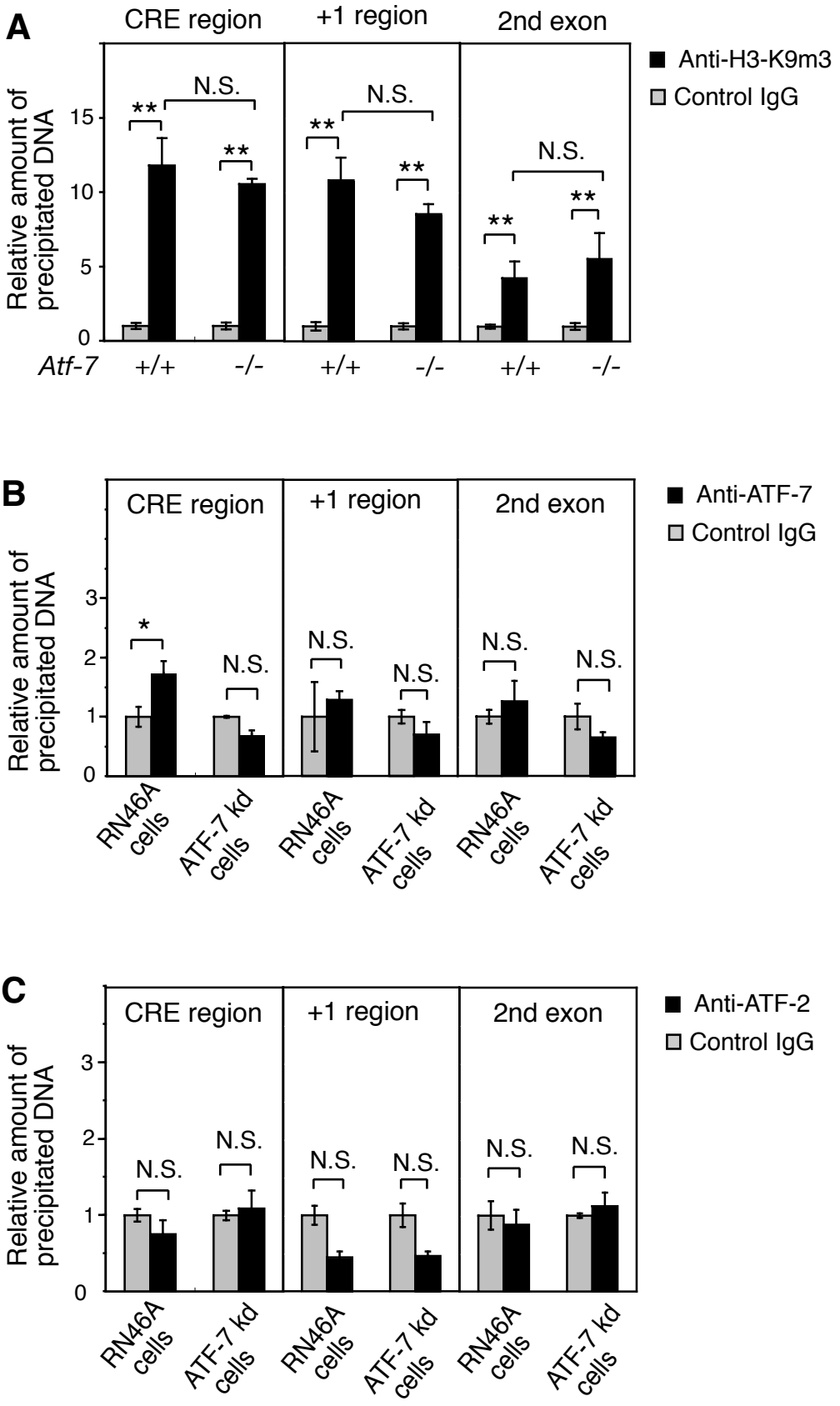
A
CRE region
+1 region
2nd exon
Anti-H3-K9m3
Control IgG
Relative amount of precipitated DNA
15
10
5
0
**
N.S.
Atf-7
+/+
-/-
B
Anti-ATF-7
Control IgG
3
2
1
0
*
RN46A cells
ATF-7 kd cells
C
Anti-ATF-2
Control IgG

Supplementary Fig. S10. Maekawa, T. *et al.*

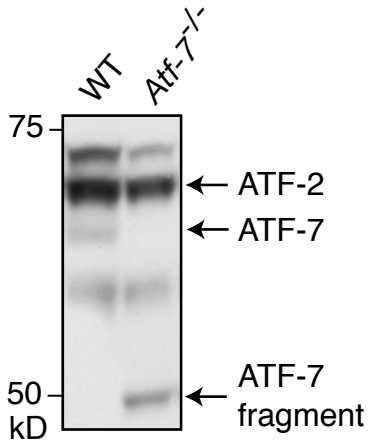

Supplementary Fig. S11. Maekawa, T. *et al*

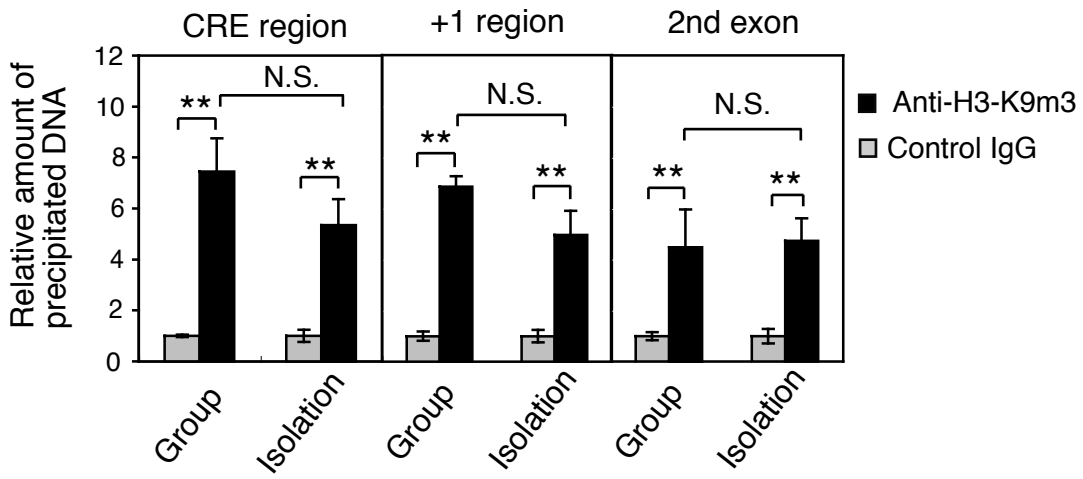

Supplementary Fig. S12. Maekawa, T. *et al*.